159. The Molecular and Crystal Structure of the Glycopeptide A-40926 Aglycone

by **Martina Schäfer, Ehmke Pohl**[1]), **Karen Schmidt-Bäse**[2]), and **George M. Sheldrick***

Institut für Anorganische Chemie der Universität Göttingen, Tammannstrasse 4, D-37077 Göttingen

and **Rolf Hermann**[3]), **Adriano Malabarba**, and **Marino Nebuloni**

Marion Merrell Dow Research Institute, Lepetit Research Center, I-21040 Gerenzano (Va)

and **Giancarlo Pelizzi**

Istituto di Strutturistica, Università di Parma, Via delle Scienze, I-43100 Parma

(11.III.96)

The crystal structure of a glycopeptide antibiotic A-40926 aglycone was investigated by X-ray analysis at −120°. A-40926 crystallises in the orthorhombic space group $P2_12_12_1$ with two monomers in the asymmetric unit, $a = 21.774(4)$, $b = 28.603(7)$, $c = 29.757(4)$ Å. 'Conventional' direct methods approach failed to solve the structure, but a novel iterative real/reciprocal space procedure was successful. Refinement against 11248 F^2 data led to $R1 = 13.3\%$ for 6770 $F > 4\sigma(F)$. The two monomers of A-40926 have similar conformations and are bound by antiparallel H-bonds to form a 'chain' structure of connecting dimers. The antibiotic molecule possesses a 'binding pocket' for the C-terminal carboxy group of the cell-wall protein, which is consistent with suggestions based on NMR data and the recently reported crystal structure of ureido-balhimycin. In A-40926 the monomers are polymerically linked by H-bonds, quite unlike the tight dimer formation observed in ureido-balhimycin.

Introduction. – A-40926 is a glycopeptide antibiotic produced by the *Actinomadura strain*. It possesses *in vitro* activity against *Gram* positive aerobic pathogens and is used to treat *Neisseria gonorrheae* [1–4]. Glycopeptides are linear heptapeptides with five aromatic residues (*Fig. 1*) [5] [6]. These aromatic side chains are covalently linked to form either diphenyl-ether bonds (residues 2 and 4) or biphenyl bonds (residues 4 and 6). Sugar residues can be attached at positions R^2, R^4, R^{10} and R^{12}. Substituents R^1 and R^3 are invariably either Cl- or H-atoms. Four different families of glycopeptides are known: vancomycin, ristocetin, avoparcin and synmonicin [7]. In ristocetin, there is a further diphenyl-ether bond between the aromatic side chains of residues 1 and 3, whereas in the other three families, residues 1 and 3 are not coupled. A-40926 is a member of the ristocetin group (*Fig. 2*) and in the aglycone, the sugar residues have been removed; R^1 is chlorine and R^3 hydrogen, and an additional Cl-atom is attached to ring F.

One common feature of all glycopeptides is their ability to form a 'binding pocket' which complexes with the D-alanine-D-alanine C-terminal cell-wall peptide called 'doc in'. Extensive NMR studies have shown that this complex is stabilised by strong intermolecular H-bonds between the C=O and amide groups [8–13].

---

[1]) Present address: Department of Biological Structure, University of Washington, Seattle, WA 98195, USA.

[2]) Present address: Max-Planck-Institut für Biochemie, D-82152 Martinsried.

[3]) Present address: Ossenkampstiege 81, D-48163 Münster.

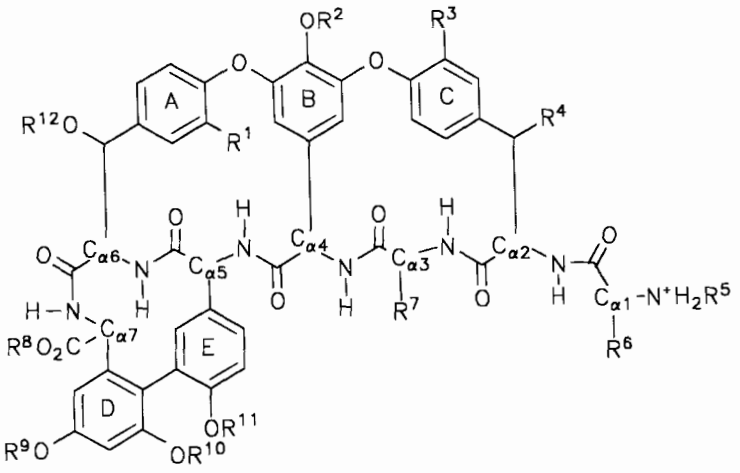

Fig. 1. *Heptapeptide structure of the glycopeptide antibiotics*

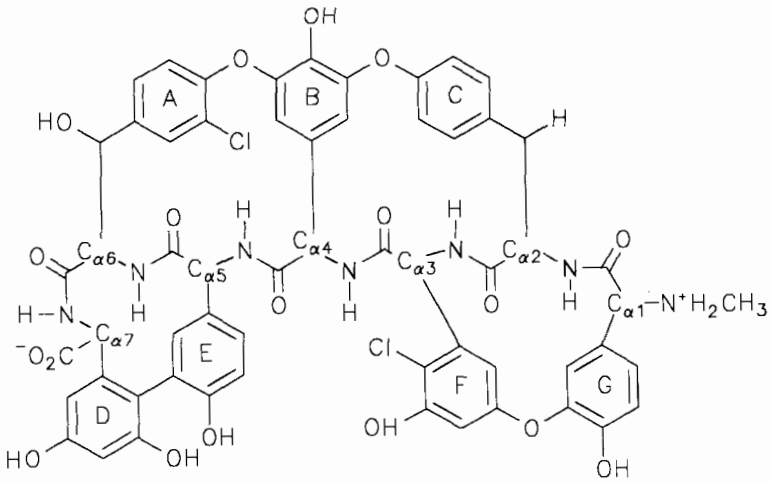

Fig. 2. *Chemical constitution of A-40926 aglycone*

The first X-ray analysis of a glycopeptide derivative, the degradation product CDP-1, was reported in 1978 [14], but this involved a ring rearrangement relative to vancomycin itself [15] [16]. The first crystal structure of a naturally occurring glycopeptide antibiotic, ureido-balhimycin, was reported recently [17]. There are three important differences between A-40926 aglycone and ureido-balhimycin. Firstly, the sugar residues have been eliminated in the aglycone, secondly, in A-40926 aglycone the aromatic side chains of residues 1 and 3 are coupled as in ristocetin and, thirdly, Cl-atom is located at residue 6 rather than 3 in ureido-balhimycin. It will be shown that these differences causes dramatic changes in the dimerization of A-40926 aglycone in comparison to ureido-balhimycin.

Here, we report the crystal structure of the A-40926 aglycone. Diffraction data were collected on a *Stoe-Siemens* four-circle dffractometer with MoK_α radiation at −120° in

1988. Conventional direct methods failed to solve the structure then, but we were recently able to solve the structure using a novel real/reciprocal space recycling procedure involving the tangent formula and peaklist optimisation [18].

Results and Discussion. – A-40926 Aglycone crystallises with two independent molecules in the asymmetric unit in the orthorhombic space group $P2_12_12_1$. Crystal data are presented in *Table 1*. The structure and numbering scheme of both molecules is shown in *Fig. 3*. All bond lengths and angles are in the expected range. Each molecule forms an open bowl where the peptide backbone is located on the bottom, and the aromatic side chains form the edges. The two molecules have similar conformations, as shown by inspection of the torsion angles given in *Table 2*. *Fig. 4* shows a least-squares fit of both molecules where all atoms were fitted except the H- and carboxy O-atoms. The r.m.s. deviation of the fitted atoms was 0.56 Å.

Table 1. *Crystal Data and Structure Refinement for A-40926*

Empirical formula	$C_{59}H_{47}Cl_2N_7O_{18} \cdot 38\ H_2O$	θ range for data collection	4.00 to 19.99
Formula weight [g/mol]	1820.94	Limiting indices	$-7 \leq h \leq 19, -26 \leq k \leq 27,$
Temperature [K]	153(2)		$-27 \leq l \leq 28$
Wavelength [Å]	0.71073	Reflections collected	12062
Crystal system	Orthorhombic	Independent reflections	11248 ($R_{int} = 0.1251$)
Space group	$P2_12_12_1$	Refinement method	Full-matrix-block
Unit cell dimensions [Å]	$a = 21.774(4)$		least-squares on F^2
	$b = 28.603(7)$	Data / restraints / parameter	11248 / 2545 / 2235
	$c = 29.757(4)$	Goodness-of-fit S[a])	1.359
V[Å^3]	18533(6)	g_1, g_2	0.2, 0.0
Z	8	Final R indices [$F > 4\sigma(F)$[b])]	$R1 = 0.1325$, $wR2 = 0.3257$
Density (calc.) [Mg/m^3]	1.357	R indices (all data)[c])	$R1 = 0.2046$, $wR2 = 0.3862$
Absorption coefficient [mm^{-1}]	0.176	Absolute structure parameter	−0.3(3)
F(000)	8032	Max. difference density [aÅ^{-3}]	0.914
Crystal size [mm]	0.3 × 0.3 × 0.2	Min. difference density [eÅ^{-3}]	−0.494

[a]) $S = [\Sigma[w(F_o^2 = F_c^2)^2]/(n-p)]^{1/2}$.
[b]) $wR2 = \{\Sigma[w(F_o^2 = F_c^2)^2]/\Sigma[w(F_o^2)^2]\}^{1/2}$; $w^{-1} = \sigma^2(F_o^2) + (g_1P)^2 + g_2P$, where $P = (F_o^2 + 2F_c^2)/3$.
[c]) $R1 = \Sigma\|F_o| - |F_c\|/\Sigma|F_o|$.

Table 2. *Selected Torsion Angles* [°]

Aromatic ether linkage	Molecule 1	Molecule 2	Aromatic ether linkage	Molecule 1	Molecule 2
			Peptide ω		
C(109)–O(103)–C(113)–C(114)	−103(1)	−103(1)	C(135)–C(137)–N(101)–C(120)	170(2)	171(2)
C(110)–C(109)–O(103)–C(113)	−9(2)	−11(2)	C(120)–C(121)–N(102)–C(122)	−171(2)	−169(2)
C(102)–O(101)–C(107)–C(112)	4(2)	9(2)	C(122)–C(138)–N(104)–C(139)	−174(1)	−173(1)
C(103)–C(102)–O(101)–C(107)	−107(1)	−108(1)	C(139)–C(140)–N(105)–C(141)	−164(1)	−158(1)
C(127)–O(106)–C(129)–C(130)	−61(2)	−46(2)	C(141)–C(142)–N(106)–C(143)	−6(2)	5(2)
C(126)–C(127)–O(106)–C(129)	167(2)	148(2)	C(143)–C(145)–N(107)–C(146)	−163(1)	−164(1)
Peptide ψ			Peptide ϕ		
N(103)–C(135)–C(137)–N(101)	−158(2)	−160(2)	C(137)–N(101)–C(120)–C(121)	74(2)	80(2)
N(101)–C(120)–C(121)–N(102)	35(2)	28(2)	C(121)–N(102)–C(122)–C(138)	−155(2)	−122(2)
N(102)–C(122)–C(138)–N(104)	−99(2)	−88(2)	C(138)–N(104)–C(139)–C(140)	145(1)	147(1)
N(104)–C(139)–C(140)–N(105)	−140(1)	−133(1)	C(140)–N(105)–C(141)–C(142)	158(1)	144(1)
N(105)–C(141)–C(142)–N(106)	−154(1)	−166(1)	C(142)–N(106)–C(143)–C(145)	−99(2)	−105(2)
N(106)–C(143)–C(145)–N(107)	148(1)	156(1)	C(145)–N(107)–C(146)–C(147)	−87(2)	−96(2)

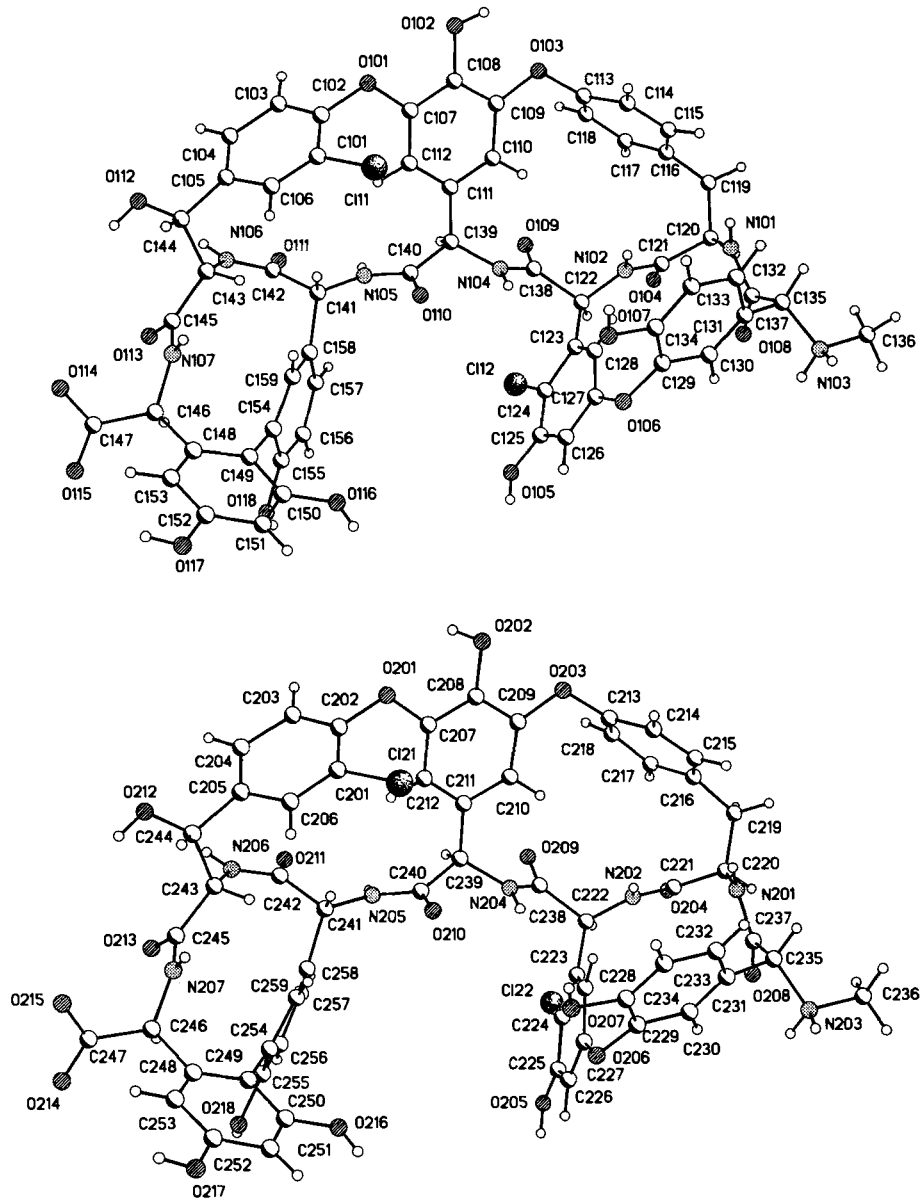

Fig. 3. *The two crystallographically independent molecules of A-40926 aglycone showing the numbering scheme*

The part of the structure containing the additional ring system between amino acids 1 and 3 possesses significantly higher anisotropic displacement parameters, indicating a higher degree of flexibility (*Fig. 5*). The same observation was made for the crystal structure of ureido-balhimycin, supporting the thesis that this part of the molecule could be the 'flap' of the binding pocket in all glycopeptides. The overall structure of the

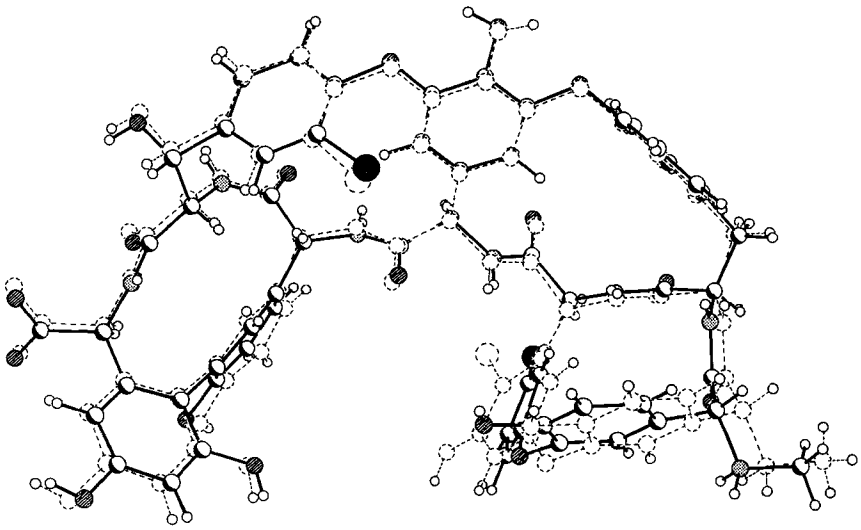

Fig. 4. *Least-squares fit of the two independent molecules*

A-40926 aglycone is very similar to the previously reported structure of ureido-balhimycin. The superposition (*Fig. 6*) shows that the backbone conformations agree well; all non-H-atoms except the vancosamine and glucose residues, and the additional aromatic system of the ristocetin group were fitted with an average r.m.s. deviation of 0.64 Å for all four monomers.

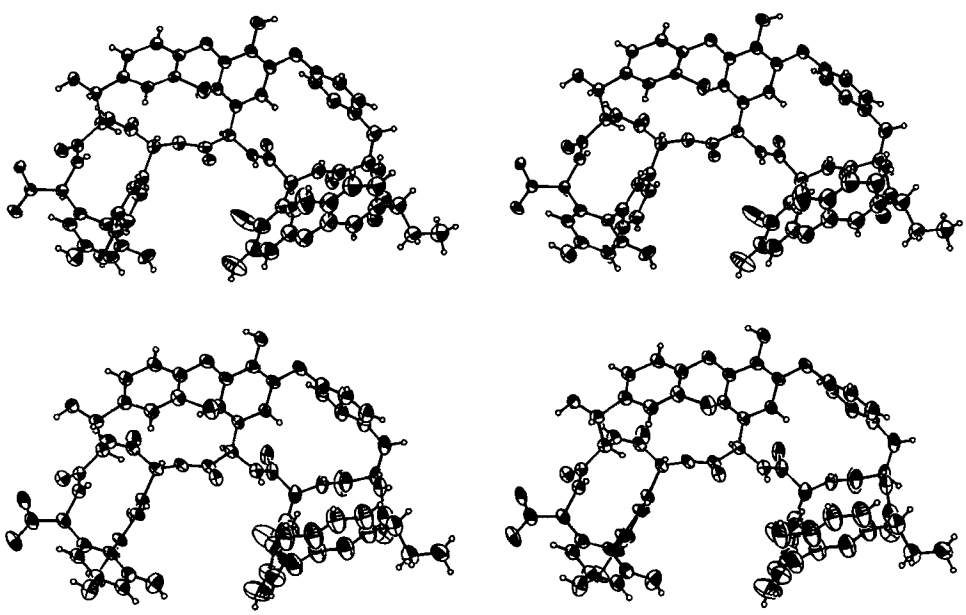

Fig. 5. *Stereoview of 50% probability anistropic displacement ellipsoids of the two independent molecules*

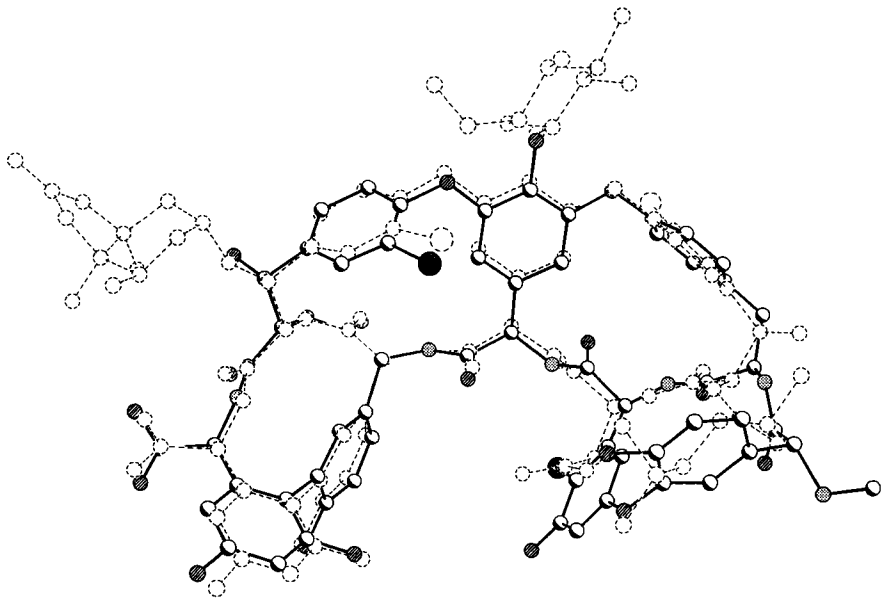

Fig. 6. *Least-squares fit of A-40926 aglycone and ureido-balhimycin*

The two independent molecules in the cell are linked together by four intermolecular H-bonds (*Fig. 7*). Firstly, the peptide backbones form an antiparallel arrangement with two (amide)NH···O(carbonyl) H-bonds (N(105)···O(211), N(205)···O(111)). Secondly, a OH group of the aromatic ring system G forms a H-bond with one O-atom of the terminal carboxy group of a symmetry equivalent of the other independent molecule (O(117)···O(214), O(217)···O(114)). Thus, the molecules link to form an infinite chain along the crystallographic *a* axis. The geometry of all intra- and intermolecular H-bonds is given in *Table 3*.

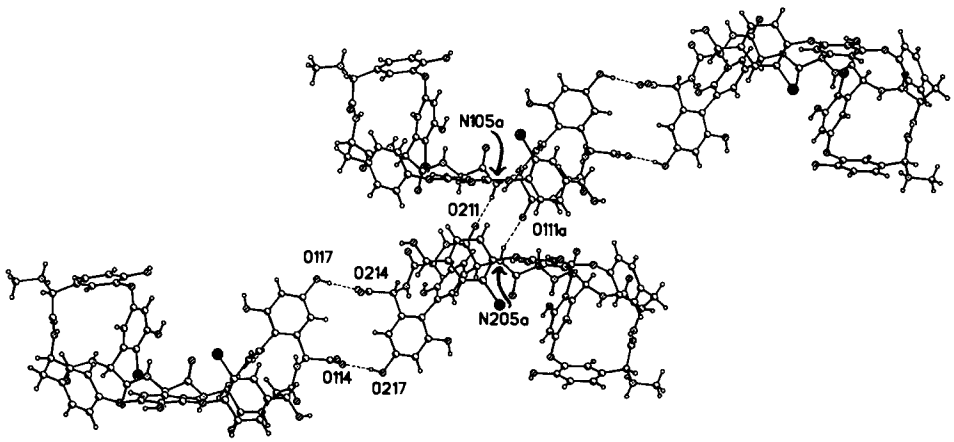

Fig. 7. *The H-bonding pattern showing the formation of chains along the crystallographic* a *axis.* $a = x + 1, y, z$.

Table 3. *Hydrogen-Bonding Geometry* [Å, °] *Involving H-Atoms That Were Included in Refinement*

H-Bonds with H···A < r(A) + 1.800 Å and < DHA > 115.0°

D–H	d(H···A)	< (D–H···A)	d(D···A)	A
O(102)–H(1O)	2.18(2)	142.5(6)	2.90(2)	O(1S(i))
N(101)–H(1N)	2.13(2)	140.1(6)	2.86(2)	O(3S)
N(102)–H(2N)	2.36(3)	156.8(7)	3.19(3)	O(31S)
O(105)–H(2O)	2.22(5)	155.6(1)	3.01(5)	O(27S)
O(107)–H(3O)	2.00(8)	149(2)	2.75(8)	O(45S)
N(103)–H(3NA)	2.00(3)	153.4(8)	2.85(3)	O(8S)
N(103)–H(3NB)	1.93(3)	153.3(9)	2.78(3)	O(13S)
N(104)–H(4N)	no H-bond formed			
N(105)–H(5N)	2.06(2)	157.0(6)	2.89(2)	O(211(ii))
N(106)–H(6N)	no H-bond formed			
O(112)–H(4O)	2.11(2)	145.5(6)	2.84(2)	O(1S)
N(107)–H(7N)	2.04(2)	167.1(7)	2.90(2)	O(5S)
O(116)–H(5O)	1.63(4)	164(3)	2.45(4)	O(44S(iii))
O(117)–H(6O)	1.79(2)	160.4(7)	2.60(2)	O(214)
O(118)–H(7O)	1.94(3)	150(1)	2.70(3)	O(26S)
O(202)–H(8O)	1.93(2)	147.9(6)	2.68(2)	O(4S)
N(201)–H(8N)	2.12(3)	151.7(7)	2.92 (3)	O(39S)
N(202)–H(9N)	2.12(3)	170.8(6)	2.99(3)	O(6S)
O(205)–H(9O)	1.88(4)	175(1)	2.72(4)	O(25S)
O(207)–H(10O)	1.75(5)	141(2)	2.47(5)	O(33S)
N(203)–H(1NA)	1.86(3)	152.3(8)	2.71(3)	O(11S)
N(203)–H(1NB)	1.92(3)	145(1)	2.73(3)	O(20S)
N(204)–H(11N)	no H-bond formed			
N(205)–H(12N)	2.19(2)	150.1(5)	2.99(2)	O(111(iv))
N(206)–H(13N)	no H-bond formed			
O(212)–H(11O)	2.00(2)	150.6(6)	2.76(2)	O(2S)
N(207)–H(14N)	2.37(3)	150.4(5)	3.17(3)	O(12S)
O(216)–H(12O)	1.87(3)	151(1)	2.64(3)	O(21S)
O(217)–H(13O)	1.81(2)	165.8(7)	2.63(2)	O(114)
O(218)–H(14O)	1.82(4)	147(2)	2.56(4)	O(34S)

(*i*) $x - 1/2, -y - 1/2, -z$; (*ii*) $x - 1, y, z$; (*iii*) $-x + 1/2, -y - 1, z - 1/2$; (*iv*) $x + 1, y, z$.

In contrast, ureido-balhimycin in the crystal forms only one dimer using two pairs of antiparallel H-bonds. A similar dimer formation has been observed in solution for other glycopeptide antibiotics by NMR technique [9–13] [19–21]. The H-bond pair of the peptide backbone in A-40926 is similar to one of the H-bond pairs in ureido-balhimycin, with nearly the same distance (N···O = 2.99 Å resp. 2.89 Å). The second H-bond pair in ureido-balhimycin is significantly longer but still in the range observed for H-bonds (N···O 3.23 Å resp. 3.14 Å) [22]. The equivalent distances in A-40926 are too long for any stabilising effect (N(106)···O(209) 3.60 Å, N(206)···O(109) 3.71 Å). One possible reason may be the additional H-bond between the vancosamine N-atom and a peptide C=O in ureido-balhimycin (N···O 3.06 Å), which could not be formed in A-40926. Because of the missing vancosamine, in A-40926 there is no possibility of such additional interaction; both antibiotic molecules possess more freedom of movement than in ureido-balhimycin. In ureido-balhimycin only one interaction between a terminal carboxy group and a OH group of the glucose residue is found (C–O···O 2.72 Å).

Most of the other atoms in A-40926 that could take part in H-bonding are on the surface of the molecule and take part in interactions (*Table 3*) with the solvent; 46 of the 76 solvent H_2O sites are in the first hydration shell and make H-bonds with the peptide. The remaining 30 are in the second shell. Only two of the polar H-atoms of each independent molecule do not appear to form H-bonds (attached to N(104), N(106), N(204) and N(206)).

In ureido-balhimycin each monomer unit forms strong H-bonds to one solvent H_2O molecule in the region of the postulated binding pocket. NMR Studies [9–13] of a vancomycin complex with Ac-D-Ala-D-Ala in aqueous solution have confirmed that the carboxy group of the dipeptide replaces this H_2O. In A-40926, only one H_2O molecule is 'housed' inside this postulated binding pocket of each molecule and forms one H-bond (N(102)···O(31S) 3.19 Å, N(202)···O(6S) 2.99 Å). The H_2O molecule attached to N(101)/N(201) is outside the binding pocket.

We thank the *Deutsche Forschungsgemeinschaft* and the *Fonds der Chemischen Industrie* for financial support.

Experimental Part

Preparation of the Aglycone and Crystal Growing. Conc. HCl (4.5 ml) was added to a stirred soln. of 5 g of A-40926 in 80 ml of DMSO and the resulting mixture heated for 9.5 h at +80°. Then, the soln. was added dropwise to 100 ml of BuOH/Et_2O 1:1 and the Et_2O phase discarded; this was repeated twice with 100 ml portions of the BuOH/Et_2O mixture. The remaining semi-solid material was dissolved in 25 ml of BuOH and precipitated with 100 ml of Et_2O. The solid product was collected by filtration. For purification, the material was dissolved in a mixture of 30 ml of H_2O and 0.6 ml of MeCN and loaded on to a column (diameter 4 cm, length 6.5 cm) filled with 40 g of silanized SiO_2. The column was washed with H_2O (*ca.* 1 l), then developed with 1.5 l of a linear gradient of 0–20% MeCN in H_2O, and eluted with 2 l of H_2O containing 20% MeCN. Crystals were obtained by slow evaporation of this soln. at r.t.

The fractions (20 ml each) containing the aglycone were pooled and evaporated to a small volume after addition of BuOH. The solid which separated after addition of Et_2O was collected, yielding 2.35 g (85.5%) of A-40926 aglycone in a fairly pure state.

Data Collection. Data were collected in 1988 on a *Stoe-Siemens-AED* four-circle diffractometer with graphite-monochromated MoK_α radiation ($\lambda = 0.71073$ Å) at −120° using a locally built low-temp. device [23]. Intensivities were obtained from $\omega/2\theta$ scan with variable scan-speed by a 'learnt profile method' [24]. 12111 reflections were measured to a maximum 2θ of 40°, of which 11248 are unique (*Friedel* opposites not merged). Further details are given in *Table 1*. Many years passed between data collection and successful structure solution. We were not able to obtain further suitable crystals, and so were not able to repeat the data collection with the improved facilities are now at our disposal.

Structure Solution. A-40926 aglycone crystallises in the orthorhombic space group $P2_12_12_1$ with two independent molecules in the asymmetric unit. With 248 independent non-H-atoms (including solvent) and relatively weak data, the structure solution using conventional direct methods was not successful. The structure was finally solved by an iterative combination of tangent formula phase expansion in reciprocal space and 'peaklist optimisation' in real space [18]. The data were expanded to space group $P1$, and 15 sets of random initial phases generated. These phases were improved by iterative cycles of tangent expansion, E-map calculation and peaklist optimisation, performed in parallel. In the peaklist optimisation, the peaks from the E-map are treated as potential atoms and are use to calculate point-atom E_c values. In two scans of the peaklist starting from the smallest peak, a peak is deleted from the list when the correlation coefficient between E_o and E_c (defined by *Fujinaga* and *Read* [25]) increases, otherwise the peak is retained.

Refinement. The structure was refined on F^2 (all data) using the program SHELXL-93 [26]. The use of restraints for geometrical and atomic displacement parameters improved the convergence of the refinement and the location of the more flexible side chains and solvent H_2O molecules. The two chemically equivalent but crystallographically independent molecules were restrained to have approximately similar 1,2 and 1,3 distances (e.s.d. 0.01 Å). This is an effective way to refine crystallographically independent molecules, because it leaves the torsion angles free to vary. For all non-H-atoms rigid-bond restraints (e.s.d. 0.002 Å^2) [27–29] were applied to the

anisotropic displacement parameters of 1,2 and 1,3 atom pairs, and the U_{ij} components were restrained to be equal (e.s.d. 0.01Å^2) of atoms closer than 1.2 Å from each other. The anisotropic displacement parameters of the solvent H_2O atoms were restrained to be approximately isotropic (e.s.d. 0.1 Å^2). The use of such restraints was essential for the success of the anisotropic refinement. 'Antibumping' restraints (e.s.d. 0.05 Å) were employed to prevent the solvent H_2O atoms from coming too close to other atoms. All H-atoms were refined using a 'riding' model. The starting positions for the OH H-atoms were those calculated by SHELXL-93 to give the best H-bonds (option AFIX 83). Because the secondary amine is very basic, and no counter-anions could be identified, the zwitterionic structure has been assumed. The refinement converged to $R1 = \Sigma (F_o - F_c)/\Sigma F_o = 0.133$ for the 6770 $F_o > 4\sigma(F_o)$ and 0.205 for all 11 248 data. The known absolute structure was assumed [4] but was not inconsistent with the value of −0.3(3) obtained for the absolute structure parameter [30] [31].

Crystallographic data (excluding structure factors) for the structure reported in this paper have been deposited with the *Cambridge Crystallographic Data Centre* as supplementary publication No. CCDC-10/23 Copies of the data can be obtained free of charge, on application to the director, CCDC, 12 Union Road, Cambridge CB2 1EZ, UK. (fax: +44 (0)1223 336033 or e-mail: teched@chemcrys.cam.ac.uk).

REFERENCES

[1] E. Selva, B.P. Goldstein, P. Ferrari, R. Pallanza, E. Riva, M. Berti, A. Borghi, G. Beretta, R. Scotti, G. Romanò, G. Cassani, V. Arioli, M. Denaro, *J. Antibot.* **1988,** *41,* 1243.

[2] B.P. Goldstein, E. Selva, L. Gastaldo, M. Berti, R. Pallanza, F. Ripamonti, P. Ferrari, M. Denaro, V. Arioli, G. Cassani, *Antimicrob. Agents Chemother.* **1987,** *31,* 1961.

[3] M.J. Robbins, D. Felmingham, G.L. Ridway, R.N. Grüneberg, in 'Progress in Antimicrobial and Anticancer Chemotherapy', Eds. B. Berkarda et al., Proceedings of the 15th ICC, Munich, Tokyo, Shanghai, 1987, pp. 326–328.

[4] J.P. Waltho, D.H. Williams, E. Selva, P. Ferrari, *J. Chem. Soc., Perkin Trans. 1* **1987,** 2103.

[5] F. Parenti, *J. Clin. Pharmacol.* **1988,** *28,* 136.

[6] J.C.J. Barna, D.H. Williams, *Ann. Rev. Microbiol.* **1984,** *38,* 339.

[7] F. Parenti, B. Cavalleri, *Drugs Future* **1990,** *15.* 57.

[8] J.P. Waltho, D.H. Williams, *J. Am. Chem. Soc.* **1989,** *111,* 2475.

[9] P. Groves, M.S. Searle, J.P. Mackay, D.H. Williams, *Structure* **1994,** *2,* 747.

[10] P. Groves, M.S. Searle, J. Chicarelli-Robinson, D.H. Williams, *J. Chem. Soc., Perkins Trans. 1* **1994,** 659.

[11] H. Molinari, A. Pastore, L. Lian, G.E. Hawkes, K. Sales, *Biochemistry* **1990,** *29,* 2271.

[12] D.H. Williams, M.P. Williamson, D.W. Butcher, S.J. Hammond, *J. Am. Chem. Soc.* **1983,** *105,* 1332.

[13] D.H. Williams, D.W. Butcher, *J. Am. Chem. Soc.* **1981,** *103,* 5697.

[14] G.M. Sheldrick, P.G. Jones, O. Kennard, D.H. Williams, G.A. Smith, *Nature (London)* **1978,** *271,* 223.

[15] C.M. Harris, H. Kopecka, Th.M. Harris, *J. Am. Chem. Soc.* **1983,** *105,* 6915.

[16] M.P. Williamson, D.H. Williams, *J. Am. Chem. Soc.* **1981,** *103,* 6580.

[17] G.M. Sheldrick, E. Paulus, L. Vertesy, F. Hahn, *Acta Crystallogr., Sect. B* **1995,** *51,* 89.

[18] G.M. Sheldrick, R.O. Gould, *Acta Crystallogr., Sect. B* **1995,** *51,* 423.

[19] J.P. Mackay, U. Gerhard, D.A. Beauregard, R.A. Maplestone, D.H. Williams, *J. Am. Chem. Soc.* **1994,** *116,* 4573.

[20] J.P. Mackay, U. Gerhard, D.A. Beauregard, M.S. Westwell, M.S. Searle, D.H. Williams, *J. Am. Chem. Soc.* **1994,** *116,* 4581.

[21] U. Gerhard, J.P. Mackay, R.A. Maplestone, D.H. Williams, *J. Am. Chem. Soc.* **1993,** *115,* 232.

[22] G.A. Jeffrey, W. Sanger, 'Hydrogen Bonding in Biological Structures', Springer-Verlag, Berlin–Heidelberg, 1991.

[23] T. Kottke, D. Stalke, *J. Appl. Crystallogr.* **1993,** *26,* 615.

[24] W. Clegg, *Acta Crystallogr., Sect. A* **1981,** *37,* 22.

[25] M. Fujinaga, R.J. Read, *J. Appl. Crystallogr.* **1987,** *20,* 517.

[26] G.M. Sheldrick, *J. Appl. Crystallogr.*, in preparation.

[27] J.S. Rollet, in 'Crystallographic Computing', Eds. F.R. Ahmed, S.R. Hall, and C.P. Huber, 1970, Copenhagen–Munskgaard, pp. 107–181.

[28] F.L. Hirshfeld, *Acta Crystallogr., Sect. A* **1976,** *32,* 239.

[29] K.N. Trueblood, J.D. Dunitz, *Acta Crystallogr., Sect. B* **1983,** *39,* 120.

[30] H.D. Flack, *Acta Crystallogr., Sect. A* **1983,** *39,* 876.

[31] G. Bernadinelli, H.D. Flack, *Acta Crystallogr., Sect. A* **1985,** *41,* 500.